An optimized infinite time-evolving block decimation algorithm for lattice systems

Junjun Xu(许军军)[†]

Institute of Theoretical Physics, University of Science and Technology Beijing, Beijing 100083, *China*

(Received 16 September 2022; revised manuscript received 16 September 2022; accepted manuscript online 19 September 2022)

The infinite time-evolving block decimation algorithm (iTEBD) provides an efficient way to determine the ground state and dynamics of the quantum lattice systems in the thermodynamic limit. In this paper we suggest an optimized way to take the iTEBD calculation, which takes advantage of additional reduced decompositions to speed up the calculation. The numerical calculations show that for a comparable computation time our method provides more accurate results than the traditional iTEBD, especially for lattice systems with large on-site degrees of freedom.

Keywords: time-evolving block decimation, matrix product states, spin models, symmetry-protected topological states

PACS: 03.67.Ac, 64.70.Tg, 75.10.Kt, 75.10.Jm **DOI:** 10.1088/1674-1056/ac92d4

1. Introduction

The success of density matrix renormalization group (DMRG) method has enormously enriched our understanding of fundamental properties of quantum matter in the last decades.[1,2] It was not until recently that the underlying reason behind its success was fully understood. Basically, it is due to the limited entanglement the system can reach.[3] In this case, the DMRG can be better understood as a variational matrix product state (MPS) ansatz.[4] Based on the MPS formula, various numerical methods are proposed, for example, the time-evolving block decimation (TEBD),[5,6] the projected entangled-pair states (PEPS),[7] and the time evolution with MPS (tMPS) algorithms.[8,9] These methods show clearer insights into the quantum states and more efficiency in the calculations.

Even though the above numerical algorithms have largely reduced the Hilbert space by choosing suitable basis and truncated bond dimensions, we can only deal with finite system size and are still far from the thermodynamic limit. Typically, we have to interpolate the results to infinite size. More recently, Vidal proposed an MPS algorithm for infinite one-dimensional chain, the infinite time-evolving block decimation algorithm (iTEBD).[10,11] The ideal is to take into account the translational invariance of the MPS formula, and the update of the whole MPS is replaced by the iteration of only several sites. This leads to a dramatic speedup of the calculation time, which is independent of system size.

The above MPS formulas provide ideal tools for the study of non-trivial systems with limited entanglement, especially for symmetry-protected topological (SPT) states. Recent researches on SPT states show interest in systems involving more on-site degrees of freedom, for example, the $SU(N)$ valence bond states with different high-dimensional representations.[12–18] In this case, even the iTEBD calculation becomes very heavy. In this paper, we propose an optimized algorithm based on the iTEBD, by carrying out reduced decompositions in the system and including as much information as possible to achieve a more efficient algorithm.

This paper is organized as follows. First, we give an introduction of the original iTEBD and show the procedure for each step. Next, we introduce our optimized method and explain why this should be valid. Then we carry out actual calculations and compare with the traditional iTEBD. Lastly, we give our summaries and mention possible following directions.

2. The basics of iTEBD and our optimized algorithm

It has been shown that the ground state of a correlated system can be written as an MPS form, given that the entanglement of the system is limited. If the ground state has translational invariance, this MPS can be written as

$$|\psi\rangle = \sum_{\{s_i\}} \cdots \Lambda\Gamma^{s_{i-1}}\Lambda\Gamma^{s_i}\Lambda\Gamma^{s_{i+1}}\Lambda\cdots|\cdots s_{i-1}s_is_{i+1}\cdots\rangle,$$

where Λ is an $m\times m$ diagonal matrix with entries of the Schmidt eigenvalues. Thus, we have $\mathrm{Tr}[\Lambda^2]=1$. The bond dimension m characterizes the degree of freedom in the virtual index, and indicates how many states are entangled for two sub-systems. The physical index s_i at site i is connected to the $m\times m$ matrix Γ^{s_i}, and has dimension d. The normalization of the MPS gives the canonical condition

$$\sum_s (\Gamma^s)^\dagger\Lambda^2\Gamma^s = \sum_s \Gamma^s\Lambda^2(\Gamma^s)^\dagger = \mathbb{1}. \tag{1}$$

For systems with only nearest neighbor interaction in iTEBD, one first writes the Hamiltonian as $H=h_\mathrm{o}+h_\mathrm{e}$, where

[†]Corresponding author. E-mail: jxu@ustb.edu.cn

© 2023 Chinese Physical Society and IOP Publishing Ltd

$h_{\rm o}$ ($h_{\rm e}$) includes only the odd (even) bonds, and the evolution operator for each time step Δt can then be written using Trotter decomposition as

$$U(\Delta t) \approx {\rm e}^{-{\rm i}h_{\rm o}\Delta t}\,{\rm e}^{-{\rm i}h_{\rm e}\Delta t}. \tag{2}$$

Figure 1 illustrates the typical procedure for a single time step acting on the even bond in iTEBD. Translational invariance ensures that the MPS has the "Γ–Λ" structure, and is described only by two sets of values "$\Gamma_{\rm e}$–$\Lambda_{\rm e}$" and "$\Gamma_{\rm o}$–Λ_0" as shown in Fig. 1.[10] After the gate $U_{\rm e} = \exp(-{\rm i}h_{\rm e}\Delta t)$ is acting on the MPS, a singular value decomposition (SVD) is carried out, resulting in the updated Schmidt eigenvalues $\tilde{\Lambda}_{\rm e}$, i.e.,

$$M_{\alpha ij\beta} = \sum_{\gamma=1}^{m} U_{\alpha i\gamma}\left(\tilde{\Lambda}_{\rm e}\right)_{\gamma\gamma}\left(V^{\dagger}\right)_{\gamma j\beta}. \tag{3}$$

To keep the basis orthonormal with nearby sites, the diagonal matrix $\Lambda_{\rm o}$ is inserted into the left and right sides of the above matrix, as shown in Fig. 1, and the two Γ matrices are updated as

$$\left(\tilde{\Gamma}_{\rm e}\right)_{\alpha i\gamma} = \left(\Lambda_{\rm o}^{-1}\right)_{\alpha\alpha} U_{\alpha i\gamma}, \tag{4}$$

$$\left(\tilde{\Gamma}_{\rm o}\right)_{\gamma j\beta} = V^{\dagger}_{\gamma j\beta}\left(\Lambda_{\rm o}^{-1}\right)_{\beta\beta}. \tag{5}$$

This finishes the evolution on the even bond, which results in the updated $\tilde{\Lambda}_{\rm e}$, $\tilde{\Gamma}_{\rm e}$, and $\tilde{\Gamma}_{\rm o}$. A similar update on the odd bond is then followed, according to the Trotter decomposition in Eq. (2), which leads to updated $\tilde{\Lambda}_{\rm o}$, $\tilde{\Gamma}_{\rm o}$, and $\tilde{\Gamma}_{\rm e}$. Iteratively updating the MPS will give the ground-state (for imaginary time) or dynamical properties of the system. Here we can find that in iTEBD the calculations are independent of the number of lattice sites. This is due to the translational invariance of the system, and in fact we are updating different sites in parallel. This makes the iTEBD more efficient to reach the thermodynamic limit.

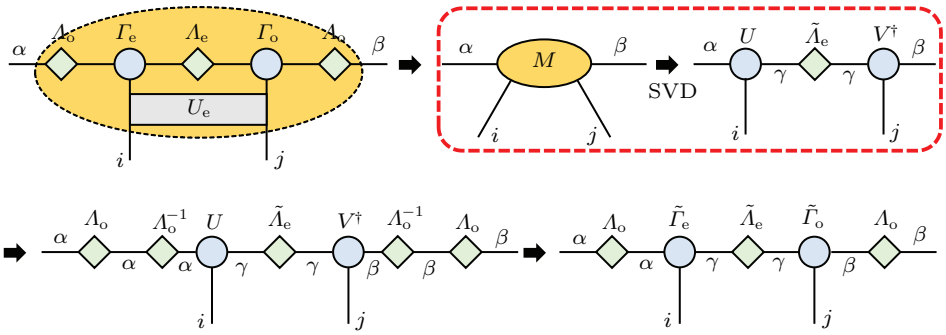


Fig. 1. A typical evolution of the MPS on the even bond in iTEBD. After the gate $U_{\rm e}$ is applied on the MPS, a singular value decomposition is carried out to get updated $\tilde{\Lambda}_{\rm e}$. A matrix inversion is then followed to get the updated $\tilde{\Gamma}_{\rm e} = \Lambda_0^{-1}U$ and $\tilde{\Gamma}_0 = V^{\dagger}\Lambda_{\rm o}^{-1}$. The matrix M is defined as the orange shaded region on the left and is decomposed according to Eq. (3), with α, β, γ the virtual indices, and i, j the physical indices.

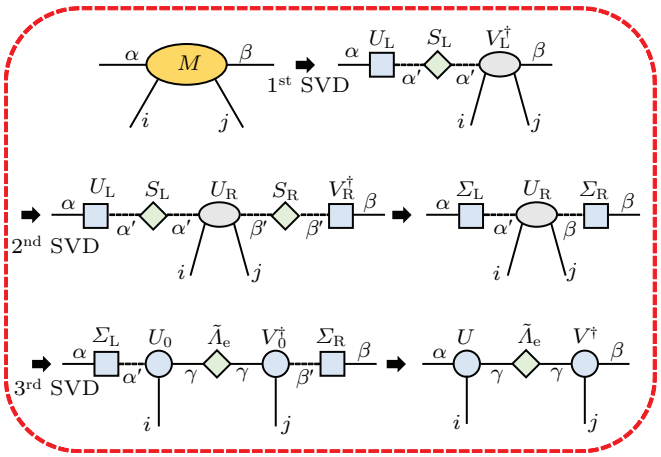


Fig. 2. An optimized decomposition scheme for the procedure circled in red in Fig. 1. We propose to speed up the final decomposition by adding two more singular value decompositions with reduced bond dimensions (dashed lines). The matrix M is decomposed according to Eq. (6), with α, α', β, β', γ the virtual indices, and i, j the physical indices.

The most time-consuming part of the above algorithm comes from the SVD process as circled by the red dashed line in Fig. 1, and the time complexity is about $O(d^3m^3)$. Thus, this algorithm will become very heavy for systems with a sufficiently large physical dimension d. One way to optimize this is to implement a reduced decomposition procedure, while trying to still keep sufficient accuracy. We summarize our proposal in Fig. 2.

Instead of the red circled procedure in Fig. 1, we add two additional reduced SVDs with bond dimension $m' < m$, as illustrated by the dashed line in Fig. 2. To fulfill this we first carry out a reduced SVD on the left virtual index as

$$M_{\alpha ij\beta} = \sum_{\alpha'=1}^{m'} \left(U_{\rm L}\right)_{\alpha\alpha'}\left(S_{\rm L}\right)_{\alpha'\alpha'}\left(V_{\rm L}^{\dagger}\right)_{\alpha' ij\beta}, \tag{6}$$

followed by a second SVD on the right virtual index as

$$\left(V_{\rm L}^{\dagger}\right)_{\alpha' ij\beta} = \sum_{\beta'=1}^{m'} \left(U_{\rm R}\right)_{\alpha' ij\beta'}\left(S_{\rm R}\right)_{\beta'\beta'}\left(V_{\rm R}^{\dagger}\right)_{\beta'\beta}. \tag{7}$$

The time complexity of the above two decompositions are $O(d^2m^3)$ and $O(\min(d^2m'm^2, d^4m'^2m))$. Now we have reduced the original matrix dimension from $dm \times dm$ to $dm' \times dm'$ and a final SVD is carried out as

$$\left(U_{\rm R}\right)_{\alpha' ij\beta'} = \sum_{\gamma=1}^{m} \left(U_0\right)_{\alpha' i\gamma}\left(\tilde{\Lambda}_{\rm e}\right)_{\gamma\gamma}\left(V_0^{\dagger}\right)_{\gamma j\beta'} \tag{8}$$

with time complexity $O(d^3m'^3)$. Finally, we arrive at the updated Schmidt eigenvalues $\tilde{\Lambda}_{\rm e}$, with

$$(U)_{\alpha i\gamma} = \sum_{\alpha'=1}^{m'} (\Sigma_{\rm L})_{\alpha\alpha'} (U_0)_{\alpha' i\gamma}, \tag{9}$$

$$\left(V^{\dagger}\right)_{\gamma j\beta} = \sum_{\beta'=1}^{m'} \left(V_0^{\dagger}\right)_{\gamma j\beta'} (\Sigma_{\rm R})_{\beta'\beta}, \tag{10}$$

where $(\Sigma_{\rm L})_{\alpha\alpha'} = \sum_{\alpha'=1}^{m'} (U_{\rm L})_{\alpha\alpha'} (S_{\rm L})_{\alpha'\alpha'}$ and $(\Sigma_{\rm R})_{\beta'\beta} = \sum_{\beta'=1}^{m'} (S_{\rm R})_{\beta'\beta'} \left(V_{\rm R}^{\dagger}\right)_{\beta'\beta}$.

The last decomposition provides a lower bound for $m' \geq m/d$, which leads to the total time complexity $O(d^2m^3 + d^2m'm^2 + d^3m'^3)$. If we consider a system with a large physical dimension d the lowest allowed value $m' = m/d$ approaches zero and the total time complexity goes to $O(d^2m^3(1 + 1/d + 1/d^2)) \approx O(d^2m^3)$. In this case, our algorithm can be of orders of magnitude faster than the original iTEBD with the time complexity $O(d^3m^3)$. For systems with a small physical dimension, e.g., for $d = 2$ and $m' = m/2$, we have time complexity $O(7m^3)$ which is still slightly smaller than the original algorithm with time complexity $O(8m^3)$. However, we have sacrificed accuracy for efficiency, as reducing the bond dimension increases the truncation error. In the following, we will check specific systems to confirm that our algorithm can lead to significant speedup with controllable accuracy, especially for a system with large physical dimensions.

3. Applications to *SU(n)* Heisenberg models

To check to what extent the above algorithm is optimized compared with the original one, we need to resort to actual calculations. In the following, we calculate the ground state energy of two SPT phases in $SU(2)$ and $SU(4)$ antiferromagnetic Heisenberg models (AFHM), respectively.

We first consider the Haldane phase in spin-1 AFHM,

$$H_2 = J \sum_i \boldsymbol{S}_i \cdot \boldsymbol{S}_{i+1} \tag{11}$$

with $J > 0$, and $\boldsymbol{S}_i = \left(S_i^x, S_i^y, S_i^z\right)$ is the spin-1 operator at site i. It is the first example of SPT phases, with an excitation gap and degenerate entanglement spectrum protected by time reversal, inversion, or D_2 symmetries.[19–22] This state is found to adiabatically connect to the Affleck–Kennedy–Lieb–Tasaki (AKLT) state.[23,24] We show a cartoon in Fig. 3 as the structure of the AKLT state, where each spin-1 site (labeled by the dashed circle) is decomposed into two spin-1/2 particles. Two spin-1/2 particles from nearest neighboring sites form a spin-singlet state as indicated by the solid line.

Figure 3 shows the ground state energy of H_2 as a function of iterations n for two different step sizes $\Delta\tau = 0.1$ and 0.01. For $\Delta\tau = 0.1$ our algorithm with bond dimension $m = 32$ and reduced one $m' = 16$ (orange solid line) shows better results than the original iTEBD with $m = 16$ (green dashed line) while with comparable time cost. However, this improvement becomes weaker when the step size is decreased to $\Delta\tau = 0.01$, as shown in the inset of Fig. 3. This indicates that the truncation error of our algorithm changes with the step size and eventually reduces the iTEBD with bond dimension $m = m'$. Nevertheless, our algorithm provides better results with comparable time cost at the beginning of a typical ground-state search with a relatively large step size. To check whether our algorithm works in a gapless system, we consider Eq. (11) with a further exchange term and goes to a gapless XY phase with $H_2' = J\sum_i \left(S_i^x S_{i+1}^x + S_i^y S_{i+1}^y\right)$. We find the results similar to the gapped SPT phase in Fig. 3 as shown in Fig. 4. Thus we expect that our algorithm should still work for gapless systems.

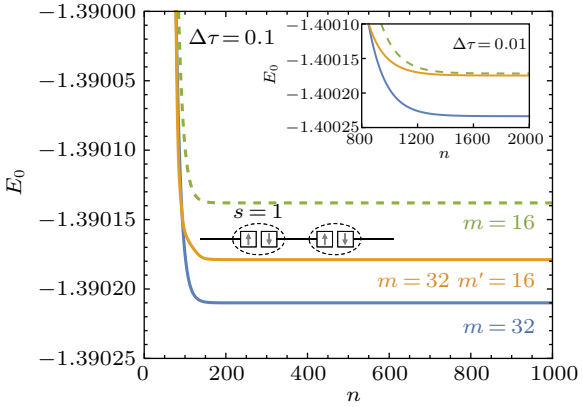


Fig. 3. The ground state energy of the spin-1 antiferromagnetic Heisenberg model H_2 as a function of iterations n for step size $\Delta\tau = 0.1$. Our algorithm (orange solid line) shows a better result compared with the original iTEBD (green dashed line), while costs comparable time. The inset shows the ground state energy for $\Delta\tau = 0.01$, where the accuracy of our algorithm is decreased.

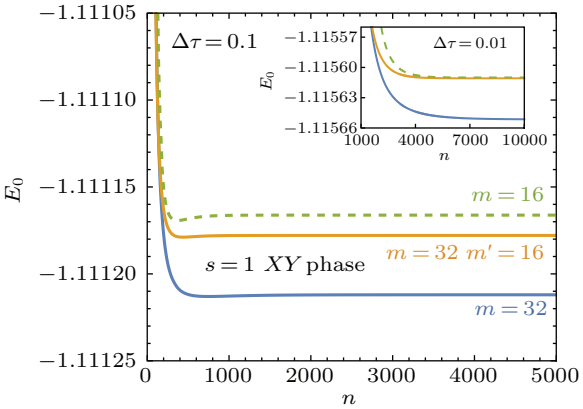


Fig. 4. The ground state energy for a spin-1 gapless XY phase with $H_2' = J\sum_i \left(S_i^x S_{i+1}^x + S_i^y S_{i+1}^y\right)$ as a function of iterations n for step size $\Delta\tau = 0.1$. Our algorithm (orange solid line) still shows a better result compared with the original iTEBD (green dashed line), and costs comparable time. The inset shows the ground state energy for $\Delta\tau = 0.01$, where the accuracy of our algorithm is decreased.

We further carry out the above calculations to a system with a larger on-site physical dimension, the 20-dimensional self-conjugate representation of the $SU(4)$ AFHM described

by

$$H_4 = J\sum_i \boldsymbol{T}_i \cdot \boldsymbol{T}_{i+1}. \tag{12}$$

Here, similar to the spin model (11), the "spin" operator $\boldsymbol{T}_i = \left(T_i^1, T_i^2, T_i^3, \ldots, T_i^{15}\right)$ is connected to the generators of $SU(4)$ with representation $[\mathbf{20}] = (0,2,0)$.[25,26] Recent studies have shown that this system has a Haldane gap.[27] The ground state of this system falls into the class-2 topological phases,[28] and is connected to the cartoon illustrated in Fig. 5. The dashed circle labels each site with the 20-dimensional representation of $SU(4)$, and the solid line connecting nearest neighbor sites indicates an $SU(4)$ singlet state.

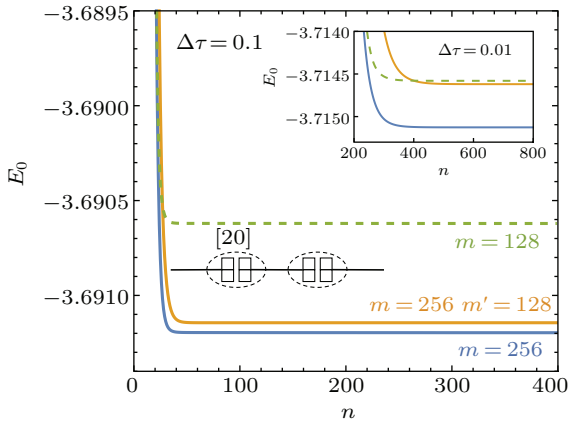


Fig. 5. The ground state energy of the $SU(4)$ antiferromagnetic Heisenberg model H_4 with self-conjugate representation $[\mathbf{20}] = (0,2,0)$ as a function of iterations n for step size $\Delta\tau = 0.1$. Our algorithm (orange solid line) shows the results very close to the original iTEBD (blue solid line), while costs time approximately an order of magnitude smaller and comparable to the reduced iTEBD (green dashed line). The inset shows the ground state energy for $\Delta\tau = 0.01$.

Similarly to Fig. 3, we present the ground state energy as a function of iterations n for two step sizes $\Delta\tau = 0.1$ and 0.01 in Fig. 5. For bond dimension $m = 256$, the results show that our algorithm with reduced bond dimension $m' = 128$ (orange solid line) has the accuracy very close to the original iTEBD with bond dimension $m = 256$ (blue solid line), yet costs time approximately an order of magnitude smaller and close to the iTEBD with $m = 128$ (green dashed line). This confirms that our algorithm becomes more powerful for systems with large single-site Hilbert space.

4. Conclusions

In summary, we have considered an optimized algorithm based on the traditional iTEBD, by introducing two additional reduced SVDs in the decomposition process. Our calculations show more accurate results for the ground state energy, compared with the traditional one for a comparable simulation time, especially for systems with large on-site degrees of freedom. This makes our method suitable for studying the SPT phases of $SU(N)$ AFHMs, and maybe even more broad systems with large on-site degrees of freedom. Finally, we mention two following directions based on our optimized algorithm. First, we can try to utilize more advanced truncation methods in the decomposition process, for example, by implementing a sampling approach.[29] Second, we can generalize this algorithm to other numerical methods, such as the infinite projected entangled-pair states in two-dimensional systems.[30]

Acknowledgement

Project supported by Fundamental Research Funds for the Central Universities (Grant No. FRF-TP-19-013A3).

References

[1] White S R 1992 *Phys. Rev. Lett.* **69** 2863
[2] White S R 1993 *Phys. Rev. B* **48** 10345
[3] Eisert J, Cramer M and Plenio M B 2010 *Rev. Mod. Phys.* **82** 277
[4] Schollwöck U 2005 *Rev. Mod. Phys.* **77** 259
[5] Vidal G 2003 *Phys. Rev. Lett.* **91** 147902
[6] Vidal G 2004 *Phys. Rev. Lett.* **93** 040502
[7] Verstraete F and Cirac J I 2004 arXiv:cond-mat/0407066 [cond-mat.str-el]
[8] Daley A J, Kollath C, Schollwöck U and Vidal G 2004 *J. Stat. Mech.: Theor. Exp.* **2004** P04005
[9] White S R and Feiguin A E 2004 *Phys. Rev. Lett.* **93** 076401
[10] Vidal G 2007 *Phys. Rev. Lett.* **98** 070201
[11] Schollwöck U 2011 *Ann. Phys.* **326** 96
[12] Greiter M, Rachel S and Schuricht D 2007 *Phys. Rev. B* **75** 060401
[13] Greiter M and Rachel S 2007 *Phys. Rev. B* **75** 184441
[14] Morimoto T, Ueda H, Momoi T and Furusaki A 2014 *Phys. Rev. B* **90** 235111
[15] Lajkó M, Wamer K, Mila F and Affleck I 2017 *Nucl. Phys. B* **924** 508
[16] Wan K, Nataf P and Mila F 2017 *Phys. Rev. B* **96** 115159
[17] Gozel S, Poilblanc D, Affleck I and Mila F 2019 *Nucl. Phys. B* **945** 114663
[18] Wamer K, Lajkó M, Mila F and Affleck I 2020 *Nucl. Phys. B* **952** 114932
[19] Haldane F D M 1983 *Phys. Lett. A* **93** 464
[20] Haldane F D M 1983 *Phys. Rev. Lett.* **50** 1153
[21] Pollmann F, Turner A M, Berg E and Oshikawa M 2010 *Phys. Rev. B* **81** 064439
[22] Pollmann F, Berg E, Turner A M and Oshikawa M 2012 *Phys. Rev. B* **85** 075125
[23] Affleck I, Kennedy T, Lieb E H and Tasaki H 1987 *Phys. Rev. Lett.* **59** 799
[24] Affleck I 1989 *J. Phys.: Condens. Matter* **1** 3047
[25] Greiner W and Müller B 1994 *Quantum Mechanics: Symmetries* (Berlin: Springer)
[26] Georgi H 1999 *Lie Algebras in Particle Physics* (Boulder: Westview)
[27] Rachel S, Thomale R, Führinger M, Schmitteckert P and Greiter M 2009 *Phys. Rev. B* **80** 180420(R)
[28] Tanimoto K and Totsuka K 2015 arXiv:1508.07601 [cond-mat.str-el]
[29] Menon A K and Elkan C 2011 *ACM Trans. Knowl. Discov. Data* **5** 13
[30] Dziarmaga J 2021 *Phys. Rev. B* **104** 094411